Gliding Arc Plasma Synthesis of Titania-based Photocatalysts: Effect of Swirl-Gas Flow Rate

Si-Yuan Zhang, Ai-Min Zhu*

Laboratory of Plasma Physical Chemistry, Dalian University of Technology, Dalian 116024, China
**Corresponding author. Email: amzhu@dlut.edu.cn (A.M. Zhu)*

Abstract: The warm plasma, generated by gliding arc discharge in vortex, with high electron density and non-equilibrium at atmospheric pressure is applied for synthesis of nano-titania catalysts. In this work, highly crystalline TiO_2 photocatalysts are one-step synthesized from the precursor of titanium tetraisopropoxide (TTIP) with air as discharge gas. X-ray diffraction (XRD) characterizations confirms that crystal phase of the as-synthesized powders is dominated by anatase and the weight fraction reaches around 80%. Transmission electron microscopy (TEM) exhibits spherical morphology of TiO_2 particles synthesized at air flow rate of 2 L/min. The lattices fringes of TiO_2 particles are also observed clearly from high resolution TEM (HRTEM). The photocatalytic activities of H_2 evolution for the synthesized TiO_2 photocatalysts are investigated.

Keywords: Air flow rate; Gliding arc discharge; Plasma synthesis; TiO_2 photocatalyst

1. Introduction

Titanium dioxide (TiO_2), because of its nontoxicity, low cost, chemical stability, and strong photoactivity, has attracted tremendous attention for its potential applications in energy conversion and environmental pollution removal[1-4]. Generally, performance of TiO_2 is closely related to characteristics of morphology, microstructure, crystalline phase and crystallinity of TiO_2, which are determined by the prepared and processed techniques[5-8]. Therefore, the synthesized methods are of importance for properties of TiO_2.

Normally, solution-based sol–gel and chemical precipitation are the common techniques for synthesis TiO_2 [7, 9-10]. However, the main deficiency is that as-synthesized products are frequently amorphous or low crystalline, which require additional heat treatments to induce crystallization. The hydrothermal method is widely employed to prepare the TiO_2 of high crystallinity[11-12] and the drawbacks of it is complex conditions and time consuming of operation. In recently, the plasma synthesis of TiO_2 powder has been received extensively interest. Thermal plasma synthesis can produce highly crystallized TiO_2, but it suffers from the disadvantages of high energy consumption, complicated quenching systems and electrode corrosion[13-16]. Simultaneously, the cold plasmas at atmospheric pressure is provided with simple device structure and well avoids the high temperature[17-18]. However, the as-synthesized TiO_2 is usually amorphous and needs to further calcination to induce crystallization. Therefore, a warm plasma generated by gliding arc discharge, which combines the advantages of thermal plasma and cold plasma, is employed. arc discharge.

The air gas flow enters reactor via tangential inlets to form vortex flow. This vortex flow drives the arc generated with the alternating current (AC) power of 41.6 kHz to gliding. Thus, a cylindrical vortex gliding arc plasma is formed. Because of its three dimensional structure, it has larger plasma area and longer residence time of reactants [19-23]. Meanwhile, it possess high electron density and high level of non- equilibrium (electron temperature greater than gas temperature)[20, 22, 24]. Therefore, it is appropriate for simple synthesis nano-titania catalysts. In this work, TTIP aerosol as the precursor of TiO_2 is carried by N_2 gas with flow rate of 100 mL/min into the plasma area. Then, the precursors are rapidly oxidized into TiO_2 powders and collected in the downstream of plasma. For the gliding arc discharge driven by gas flow, gas flow rate is a factor of great concern. Therefore, effect of the air flow rates on the characteristics of as-synthesized TiO_2 is investigated. The physic-chemical properties of as-synthesized TiO_2 were characterized. The synthesized TiO_2 samples are designated as S1, S2, and S3 corresponding to the F_{air} of 2 L/min, 3 L/min, and 4 L/min with input power of 100 W, respectively.

2. Results and discussions

The waveforms of discharge voltage and current are shown in Figure 1A and B, respectively. The discharge voltage shows sinusoidal waveform for the 2 L/min and 4 L/min. However, discharge current deviates from the sinusoidal waveform and manifests a triangle-like waveform. The photographs of the discharge are shown in Figure 1C and D. When the air flow is 2 L/min, the arc glides along the fringes of the grounded and powered electrode toward the direction of orange arrow in Figure 1C. The appearance of discharge area is cylindrical. There has obvious colour distinction between combustion of TTIP and the plasma channels. A white colour area of the combustion of TTIP located in the centre of reactor and that is surrounded by the pale red arc column. When the air flow increases to 4 L/min, the

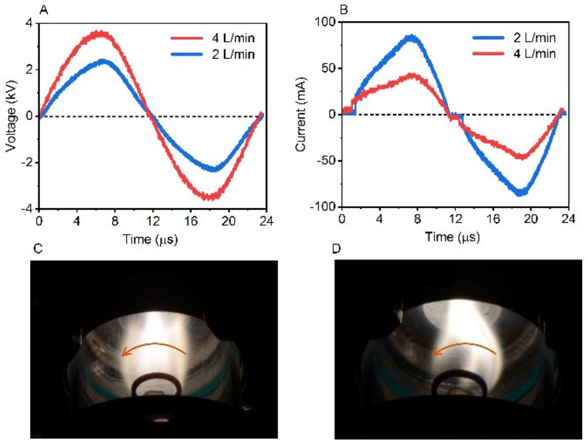

Fig. 1. Waveforms of discharge (A) voltage and (B) current and corresponding discharge photographs of (C) 2 L/min and (D) 4 L/min with exposure time of 0.2 s under input power of 100 W.

arc column is compressed toward the central by the gas flow from up to down. There gives rise to mixing between the central combustion of TTIP and arc column as shown in Figure 1D.

The crystalline phase of synthesized TiO_2 is analyzed by the X-ray diffraction (XRD). Figure 2A shows that anatase and rutile are observed in all three sample. The peaks of anatase phase (101), (004), (200), (105), (211), (204) and (116) appear, respectively. Peaks of rutile phase (110), (110) and (111) are also present. From the XRD patterns, weight fraction of the anatase f_A is approximately 80% as shown in Figure 2B. F_{air} have no obvious effect on the weight fraction of the anatase. Meanwhile, crystalline size d_A of anatase tends to decrease with the increase of F_{air}. This is also related with the residence time of the particles of TiO_2. At the large flow rate, TiO_2 particles or clusters experience a rapid quenching process and have not enough time to aggregation.

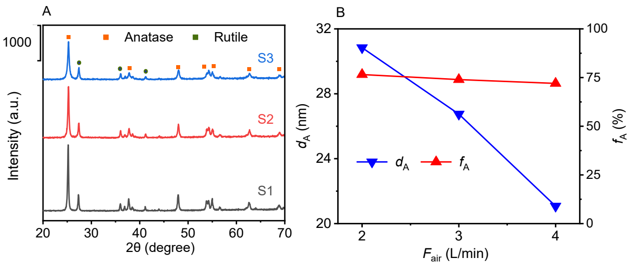

Figure. 2. XRD patterns (A) and the effect of the F_{air} on the f_A and d_A (B) of the S1, S2 and S3

The morphology and lattices fringes of S1 sample are shown in Figure 3. Particles of S1 mainly manifest spherical morphology as shown in Figure 3A. The spherical morphology of S1 can be explained by the vapour-liquid-solid (VLS) mechanism. At the lower F_{air}, the droplets consisting of liquid TiO_2

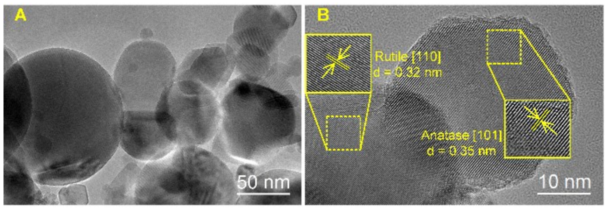

Figure. 3. TEM image (A) and HRTEM image (B) of S1 (lattice fringes in the inset).

molecular or clusters first are formed from the TTIP vapour owing to the high temperature of arc channel which is higher than melting point of TiO_2 (2143 K)[21, 26]. Subsequently, the TiO_2 droplets are fast quenched and crystallize into the spherical particle; moreover, the large spherical particle is caused by mutual collision and agglomeration of small droplets. The lattices fringes of S1 are shown in Figure 3B. Anatase and rutile crystal phases appear in S1. That is consistence with the XRD results. It is further indicated that synthesized TiO_2 through gliding arc plasma with one-step exhibits the mixed crystal.

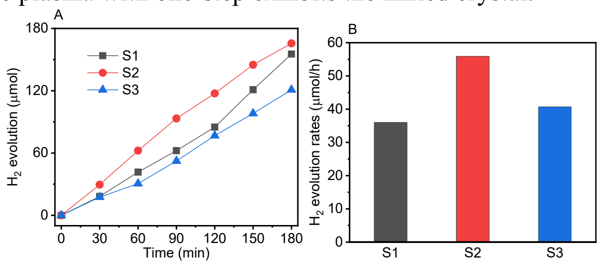

Figure. 4. Photocatalytic activity (A) and H_2 evolution rates (B) of S1, S2 and S3.

Figure 4 illustrates the photocatalytic activities of as-synthesized samples. It is obvious that the photocatalytic activities increase first and then decrease in the order of S1, S2 and S3. S2 shows the highest photocatalytic activities and H_2 evolution rate. The reason may be as follows. With air flow increasing, the energy density and the residence time gradually decrease. On the one hand, decrease of energy density and the residence time will lead to a gradual decrease in particle size and increase in specific surface area of as-synthesized TiO_2. that has positive effect on the photocatalytic activity. On the other hand, decrease of energy density and the residence time leads to gradual retention of the carbonaceous species on the surface of TiO_2 particles caused by insufficient time and energy for complete oxidation. That has negative effect on the photocatalytic activity. Therefore, the highest photocatalytic activity of S2 is result of the balance of interaction of these two factors.

In summary, highly crystalline TiO_2 is one-step prepared from TTIP aerosol through a vortex gliding arc plasma. The as-synthesized TiO_2 has a weight ratio of anatase to rutile of approximately 80/20. The morphology of S1 is dominated by the spherical and lattice fringes of anatase and rutile are all observed in HRTEM. Photocatalytic activities of H_2 evolution manifest increase first and then decrease.

Acknowledgements

This work is supported by National Natural Science Foundation of China (Grant No. 11475041).

Reference

[1] Hoffmann Michael R.,Choi Wonyong..Bahnemann Detlef W., Environmental Applications of Semiconductor Photocatalysis. Chemical Reviews **95**, 69 (1995).
[2] Diebold Ulrike, The surface science of titanium dioxide. Surface Science Reports **48**, 53 (2003).
[3] Lin Chiu Hsun,Chao Jiunn Hsing,Liu Chun Hsuan,Chang Jui Chun.Wang Feng Chieh, Effect of Calcination Temperature on the Structure of a Pt/TiO_2 (B) Nanofiber and Its Photocatalytic Activity in Generating H_2. Langmuir the Acs Journal of Surfaces & Colloids **24**, 9907 (2008).
[4] Chen Xiaobo,Shen Shaohua,Guo Liejin.Mao Samuel S., Semiconductor-based Photocatalytic Hydrogen Generation. Chemical Reviews **110**, 6503 (2010).
[5] Thompson T. L..Yates Jr Jt, Surface science studies of the photoactivation of TiO_2-new photochemical processes. Chemical Reviews **38**, 4428 (2006).
[6] Han Xiguang,Kuang Qin,Jin Mingshang,Xie Zhaoxiong.Zheng Lansun, Synthesis of Titania Nanosheets with a High Percentage of Exposed (001) Facets and Related Photocatalytic Properties. Journal of the American Chemical Society **131**, 3152 (2009).
[7] Macwan D. P.,Dave Pragnesh N..Chaturvedi Shalini, A review on nano-TiO_2 sol–gel type syntheses and its applications. Journal of Materials Science **46**, 3669 (2011).
[8] Sambandam Balaji,Surenjan Anupama,Philip Ligy.Pradeep Thalappil, Rapid Synthesis of C-TiO_2: Tuning the Shape from Spherical to Rice Grain Morphology for Visible Light Photocatalytic Application. Acs Sustainable Chemistry & Engineering **3**, 150602130745000 (2015).
[9] Sugimoto T..Zhou X., Synthesis of uniform anatase TiO_2 nanoparticles by the gel-sol method 2. Adsorption of OH^- Ions to $Ti(OH)_4$ gel and TiO_2 particles. Journal of Colloid and Interface Science **252**, 347 (2002).
[10] Sugimoto Tadao,Zhou Xingping.Muramatsu Atsushi, Synthesis of uniform anatase TiO_2 nanoparticles by gel–sol method 4. Shape control Journal of Colloid and Interface Science **259**, 53 (2003).
[11] Zhang Y. X.,Li G. H.,Jin Y. X.,Zhang Y.,Zhang J..Zhang L. D., Hydrothermal synthesis and photoluminescence of TiO_2 nanowires. Chemical Physics Letters **365**, 300 (2002).
[12] Zhang Qinghong.Gao Lian, Preparation of Oxide Nanocrystals with Tunable Morphologies by the Moderate Hydrothermal Method: Insights from Rutile TiO_2. Langmuir **19**, 967 (2003).
[13] Li J. G.,Ikeda M.,Ye R.,Moriyoshi Y..Ishigaki T., Control of particle size and phase formation of TiO_2nanoparticles synthesized in RF induction plasma. Journal of Physics D: Applied Physics **40**, 2348 (2007).
[14] Li Mingwei,Gonzalez-Aguilar José.Fulcheri Laurent, Synthesis of titania nanoparticles using a compact nonequilibrium plasma torch. Japanese Journal of Applied Physics **47**, 7343 (2008).
[15] Yong Cheol Hong.Han Sup Uhm, Production of Nanocrystalline TiO_2 Powder by a Microwave Plasma-Torch and Its Characterization. Thin Solid Films **517**, 4052 (2009).
[16] Seo Jun-Ho.Hong Bong-Guen, Thermal Plasma Synthesis of Nano-Sized Powders. Nuclear Engineering and Technology **44**, 9 (2012).
[17] Chen Chienchih,Bai Hsunling,Chein HungMin.Chen Tzu Ming, Continuous Generation of TiO_2Nanoparticles by an Atmospheric Pressure Plasma-Enhanced Process. Aerosol Science and Technology **41**, 1018 (2007).
[18] Nie Long-Hui,Shi Chuan,Xu Yong,Wu Qing-Hao.Zhu Ai-Min, Atmospheric Cold Plasmas for Synthesizing Nanocrystalline Anatase TiO_2 using Dielectric Barrier Discharges. Plasma Processes and Polymers **4**, 574 (2007).
[19] Kalra Chiranjeev S.,Cho Young I.,Gutsol Alexànder,Fridman Alexander.Rufael Tecle S., Gliding arc in tornado using a reverse vortex flow. Review of Scientific Instruments **76**, 025110 (2005).
[20] Gangoli S. P.,Gutsol A. F..Fridman A. A., A non-equilibrium plasma source: magnetically stabilized gliding arc discharge: I. Design and diagnostics. Plasma Sources Science and Technology **19**, 065003 (2010).
[21] Liu Shi-Xin,Li Xiao-Song,Zhu Xiaobing,Zhao Tian-Liang,Liu Jing-Lin.Zhu Ai-Min, Gliding Arc Plasma Synthesis of Crystalline TiO_2 Nanopowders with High Photocatalytic Activity. Plasma Chemistry and Plasma Processing **33**, 827 (2013).
[22] Zhao Tian Liang,Xu Yong,Song Yuan Hong,Li Xiao Song,Liu Jing Lin,Liu Jin Bao.Zhu Ai Min, Determination of vibrational and rotational temperatures in a gliding arc discharge by using overlapped molecular emission spectra. Journal of Physics D: Applied Physics **46**, 345201 (2013).
[23] Zhao Tian-Liang,Liu Jing-Lin,Li Xiao-Song,Liu Jin-Bao,Song Yuan-Hong,Xu Yong.Zhu Ai-Min, Temporal evolution characteristics of an annular-mode gliding arc discharge in a vortex flow. Physics of Plasmas **21**, 053507 (2014).
[24] Fridman Alexander,Nester Sergei,Kennedy Lawrence A.,Saveliev Alexei.Mutaf-Yardimci Ozlem, Gliding arc gas discharge. Prog.energy Combust.sci **25**, 211 (1999).
[25] Sing K. S. W, Reporting Physisorption Data for Gas/Solid Systems-With Special Reference to the Determination of Surface Area and Porosity. Pure & Applied Chemistry **57**, 603 (1985).
[26] Li Yali.Ishigaki Takamasa, Thermodynamic analysis of nucleation of anatase and rutile from TiO2 melt. Journal of Crystal Growth **242**, 511 (2002).